Chemistry of Natural Compounds, Vol. 38, No. 3, 2002

SYNTHESIS, STRUCTURE, AND MEMBRANE ACTIVITY OF NEW GLYCYRRHETIC ACID DERIVATIVES

B. A. Salakhutdinov,[1] D. N. Dalimov,[1] T. F. Aripov,[1]
I. I. Tukfatullina,[1] R. Kh. Ziyatdinova,[1] A. Zh. Dzhuraev,[1]
F. G. Kamaev,[1] L. Yu. Izotova,[1] B. T. Ibragimov,[1]
I. Mavridis,[2] and P. Giastas[2]

UDC 547.942: 352.465

Derivatives of 3-O-acetyl-18-βH-glycyrrhetic acid were synthesized. Their structures and membrane activities were studied.

Key words: glycyrrhetic acid derivatives, x-ray structure analysis, DSC, BLM, EPR.

The biological activity of glycyrrhizic acid and its aglycone, glycyrrhetic acid, has been studied thoroughly. However, the reasons for their wide spectrum of action are not fully understood [1-5]. The biological activity of these compounds may be due to their membrane activities including the capability to modify selectively the structure and permeability of biological membranes [3, 4, 6, 7]. There are at least two possibilities for this.

The cellular response to the action of chemical compounds may be a result of their interaction with certain membrane proteins, i.e., targets (similar to receptor interaction). Changes in the physicochemical properties of these may be the reason for the initiation or completion of intracellular biochemical reactions.

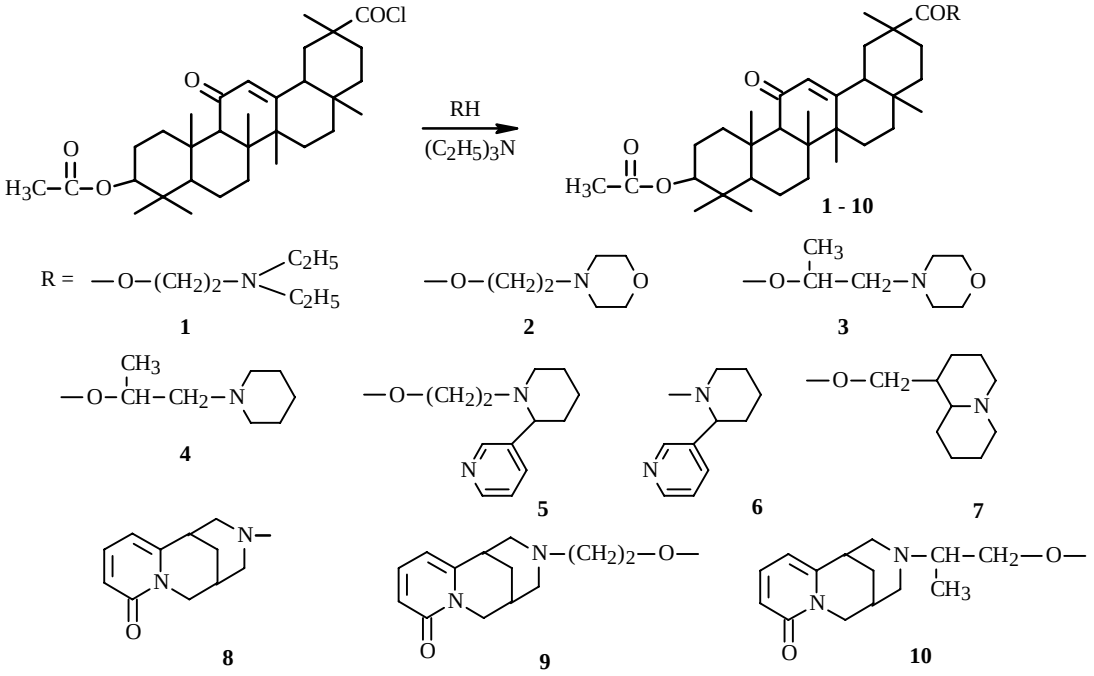

1) A. S. Sadykov Institute of Bioorganic Chemistry, Academy of Sciences of the Republic of Uzbekistan, Tashkent, ul. Akad. Abdullaeva, 83, fax (99871) 162 70 71; 2) Institute of Physical Chemistry, Scientific-Research Center "Demokritos" (Greece), 15310 AGHIA Paraskevi, Athens, Greece. Translated from Khimiya Prirodnykh Soedinenii, No. 3, pp. 209-215, May-June, 2002. Original article submitted January 28, 2002.

0009-3130/02/3803-0249$27.00

TABLE 1. Asymmetry Parameters for Rings in **8**

	Ring						
A. p.*	A	B	C	D	E	F	G
DC_2	3.8 (C2-C3)	5.3 (C5-C6)		7.6 (C13-C14)	4.3 (C18-C19)	2.6 (C34-C-35)	
DCs	0.4 (C2)	3.5 (C5)	2.3 (C8)	4.0 (C13)	3.9 (C18)	0.4 (C35)	2.6 (C35)
φ	54.2	53.6	39.2	46.5	51.8	57.4	43.0

*Asymmetry parameters

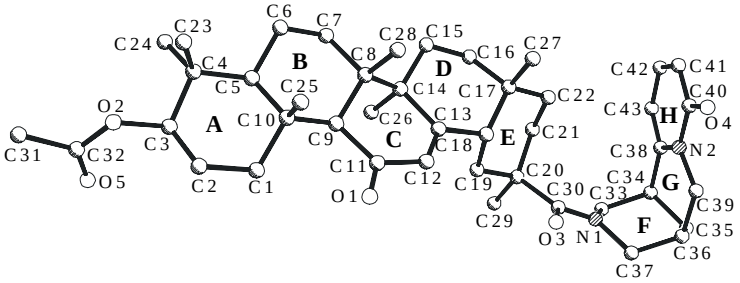

Fig. 1. Molecular structure of N-(3-β-acetoxy-11,30-dioxo-18β-olean-12-en-30-yl)cytisine (**8**).

The other possibility involves the interaction of membrane-active molecules with the lipid matrix of biological membranes. As a result of this the structural-dynamic parameters of lipid molecules (packing, orientation, charge state, etc.) may change. Also, the membrane conductivity for various ions (K^+, Na^+, Ca^{2+}, Mg^{2+}) may change. Eventually this destroys the ionic homeostasis of the cell.

Therefore, we investigated the membrane activities of several newly synthesized amides and esters of 3-O-acetyl-18βH-glycyrrhetic acid.

Derivatives of 3-acetoxyglycyrrhetic acid **1**-**10** were prepared by reacting the acylchloride of this acid with the appropriate amines and aminoalcohols in the presence of triethylamine as an acceptor for HCl.

PMR spectra of the synthesized compounds were recorded and used to characterize the structures. The base of the synthesized compounds is 3-O-acetyl-18βH-glycyrrhetic acid, for which the most characteristic signals have been assigned [13, 14]. At weak field, the signal for H-12 appears at 5.63 ppm; a multiplet for H_a-3, at 4.42 ppm. The singlet for equatorial proton H_e-1 is shifted out of the methylene region and appears as an asymmetric doublet at 2.76 ppm with J = 13.5 Hz because of the deshielding effect of the carbonyl on C-11. The solitary peak at 2.33 ppm belongs to H-9. The 3H singlet at 2.01 ppm is certainly the signal for the C-3 acetate methyl. Unresolved signals for the triterpene framework of the molecule and singlets for the seven quaternary methyls are found at strong field. Their individual assignments have been previously reported [8, 13, 14].

The PMR spectra of **1**-**10** include the signals mentioned above and those characteristic of the added substituents. Qualitative and quantitative analyses of the signals are consistent with spectra of the proposed structures.

Syntheses of **2**, **4**, **5**, and **7** have been published [8]. The physicochemical properties of the new compounds and their PMR spectra are reported in the Experimental section.

A full x-ray structure analysis (XSA) of **8** was performed. The compound consists of two parts, the triterpene (rings A, B, and C) and the cytisine (rings F, G, and H) (Fig. 1).

Rings A/B, B/C, and C/D are *trans*-fused; D/E, *cis*. Rings A, B, D, and E have the chair conformation; C, half-chair. The asymmetry parameters characterizing the degree of deviation of a given conformation from the ideal value were calculated using the program RING [9] and are listed in Table 1.

Rings F and G in the cytisine have the chair and half-chair conformations, respectively. Ring H is planar within 0.02 Å.

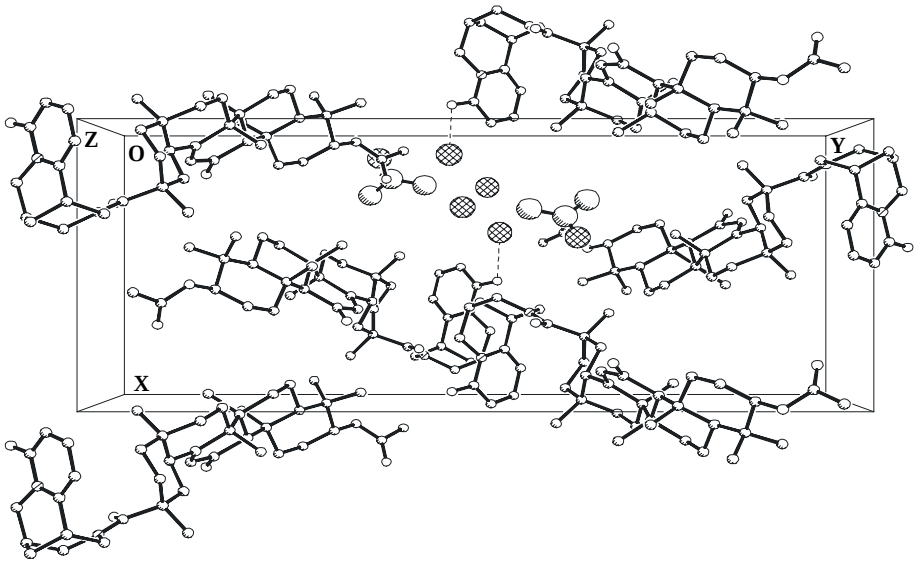

Fig. 2. Crystal structure of **8**.

The crystal structure of **8** includes acetone and water of solvation. The asymmetric unit consists of one molecule of **8**, one acetone, and two waters. The host molecule lacks proton-donating groups. Therefore, the acetone does not form H-bonds to it and is disordered over two positions with different occupancy factors (0.70 and 0.30 for the dominant and minor ones, respectively). One of the waters forms a H-bond with **8**, O1W–H...O4 of length 2.72 Å. The other water is held in the crystal structure by van-der-Waals forces (Fig. 2). The crystal structure shows that the structure is rather loosely packed even after adding the waters and acetone (density only 1.10 g/cm^3).

The membrane activities of the synthesized compounds were studied by observing their interaction with the lipid matrix of bilayer model systems. We used differential scanning microcalorimetry (DSC), electron paramagnetic resonance (EPR), and conductivity measurements of planar bilayer lipid membranes (BLM).

The model systems for the DSC study were multilamellar dispersions of dimyristoylphosphatidylcholine (DMPC), a synthetic analog of lecithin, the principal structural component of the lipid matrix of biomembranes. During cooperative melting (transition from the liquid-crystalline state to a gel), rotation around C–C bonds of acyl chains at a clearly defined temperature (T_p), called the temperature of the principal phase change, destroys the rigid packing of the lipid molecules. The melting thermogram of multilamellar DMPC dispersions exhibits a maximum at 24.1°C with a half-width of 0.8°C. A change of T_p and the peak half-width ($1/2\Delta T_p$) provides an indication of whether any factors have disturbed the cooperative melting process [10]. If membrane-active molecules insert into the interchain space of the lipid bilayers, then they perturb the fundamental packing of the lipids. As a result, some of the DMPC molecules may be excluded from the cooperative melting process or T_p may decrease because of the decreased energies of acyl interchain interactions. This destroys the cooperativity.

The relative concentration of the studied compounds in the lipid multilamellar dispersions is high and far from physiological values. We used high concentrations in order to achieve our goal of revealing the nature and properties of the interaction between the membrane-active and lipid molecules. The guest molecules may be randomly distributed in the bilayer. This can perturb the local microenvironment of the lipids, which are fully or partially (depending on the depth of intercalation of the membrane-active molecules) excluded from the cooperative melting process. As a result, T_p decreases.

Regions of increased concentration arise if the membrane-active molecules are distributed unevenly in the bilayer or on its surface [10]. The thermodynamic properties of the lipids are different in these parts and in parts free of the studied compounds. This is seen in the thermograms as a high- or low-temperature shoulder on the main melting curve. In fact, this phenomenon was observed for practically all compounds that we studied.

The values of $1/2\Delta T_p$ increased and those of T_p decreased characteristically for bilayers treated with the compounds (Table 2).

TABLE 2. Temperatures and Half-Widths* of Principal Phase Change (T_p) of DMPC Multibilayers after Addition of Studied Compounds (DMPC Concentration 300 μM)

Concentration, μM	Compound									
	1	**2**	**3**	**4**	**5**	**6**	**7**	**8**	**9**	**10**
					Temperature					
0	24.1	24.1	24.1	24.1	24.1	24.1	24.1	24.1	24.1	24.1
6	23.6	24.05	23.4	23.5	23.7	23.6	23.6	24.1	24	23.5
12	23.5	24	23.2	23.2	22.7	23.2	22.5	24.05	23.8	22.9
18	23	23.95	23.2	22.8	22.7	22.5	22.5	24	23	
					Half-width					
0	0.8	0.8	0.8	0.8	0.8	0.8	0.8	0.8	0.8	0.8
6	1.1	1.1	1.6	2.2	1.5	1.2	1.7	1.1	1.4	1.4
12	1.3	1.2	1.7	1.8	2.5	2.2	3	3.1	1.5	1
18	2.2	1.4	2	2.2	2.6	2.7	3.2	1.5	1.6	

*($1/2\ \Delta T_p$).

It was interesting to determine to what degree T_p and $1/2\Delta T_p$ depend on the structure of the membrane-active molecules. Thus, we used **2** and **3**, which differ by the presence of a methyl instead of a hydrogen in the ethylene bridge of **3**, as examples. Even at low concentrations, T_p decreases by 0.7°C and $1/2\Delta T_p$ increases by 0.8°C compared with the control. Using **3** and **4** as examples shows that replacing the morpholine "head" by piperidine in **4** also reduces T_p by 0.4°C and raises $1/2\Delta T_p$ by 0.2°C compared with the values for **3**. Modifying the environment of the N atom (**1**, **5**, **7**) changes significantly T_p and $1/2\Delta T_p$. Derivative **7** causes the greatest increase in $1/2\Delta T_p$, 1.0°C compared with **1**.

An interesting trend in the change of T_p is seen for the series **8**-**10**. Increasing the concentration of **8** has no effect on T_p whereas introducing ethyl and isopropyl bridges significantly decreases T_p. Such a trend is not observed for the half-width values.

Thus, increasing the hydrophobicity of the compound strengthens its membrane activity. Apparently the studied compounds at low relative concentrations are evenly distributed in lipid bilayers. At high concentrations they tend to form compound—lipid microdomains, the thermodynamic properties of which differ from those of lipids that are not treated with membrane-active molecules.

Spin probes can be used to determine the effect of membrane-active molecules on the orientation and motion of phospholipid acyl chains along the bilayer hydrophobic profile [11]. We used the spin probe benzo-γ-carboline, which is distributed over a different level of the bilayer hydrophobic region. Changes in the EPR spectrum provide indirect information about the effect of the membrane-active molecule on the membrane [12].

The starting EPR spectrum of the benzo-γ-carbline probe is a superposition of signals from probes located in the lipid matrix and those for which the nitroxyl group is located in an aqueous microenvironment. The determination of the distribution of probes at the membrane—water interface is yet another means of estimating the penetration of the studied molecules into the bilayer because the probes will be expelled into the aqueous phase if the distribution coefficient of the compounds at the interface is greater than that of the probe.

Let us examine the results for **8**-**10**, which have similar structures. The redistribution of probes at the membrane—water interface as the concentration of the compounds increases is shown in Fig. 3a.

We estimated the redistribution by using the quantity $k = I_A/I_M$, where I_A and I_M are the signal amplitudes for probes located in the aqueous and lipid phases, respectively. Curves were constructed in relative units compared with controls ($P = k/k_0$, where k is the experimental sample and k_0 is the control). The ability of the compounds to expel probes followed the order **8** < **9** < **10**, i.e., decreasing length of the substituent on the cytisine N atom.

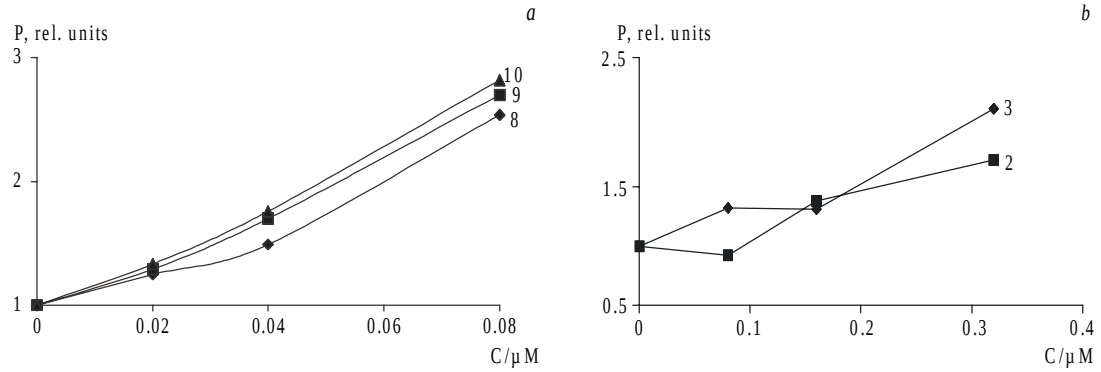

Fig. 3. Change of spin-probe distribution in lipids after addition of studied compounds (**2**, **3**, **8**-**10**).

The EPR spectra of the cytisidine derivatives have shown that the low-field peak of the probe signal in the lipid phase shifts to high-field as the concentrations of the studied compounds are increased. This is consistent with a weak disordering effect of these compounds on the initial organization of the lipids in the bilayer.

Figure 3b shows the change of probe distribution at the interface caused by **2** and **3**. The effects caused by them are similar to those mentioned above.

Thus, the EPR data lead to the conclusion that the studied compounds interact with lipid bilayers by inserting into the hydrophobic region and perturbing the initial structural organization, at least in their microenvironment.

It is interesting to compare the EPR and DSC data for the cytisine derivatives (**8**-**10**). We list the relative T_p, $1/2\Delta T_p$, and D values for final concentrations of added compounds compared with those for controls.

Compound	T_p-T_p°C	ΔT_p-ΔT_p°C	P
8	-1±0.1	0.7±0.1	2.56
9	-1.4±0.1	2.0±0.1	2.73
10	-1.75±0.1	2.6±0.1	2.84
Control	0	0	1

It can be seen that increasing the length of the hydrocarbon substituent on the cytisine N atom increases the perturbing effect of these compounds in the order **10** > **9** > **8**. Unfortunately, we could find no rigid correlation between the structures of the substituents and the changes in the spectral parameters for the other compounds.

Membrane-active molecules can change the physical properties of lipid bilayers to make them more permeable to various inorganic ions. We studied the effect of the glycyrrhetic acid derivatives on the conductivity of planar BLM.

We found that adding **1**-**3**, **5**, and **7**-**10** at concentrations up to 100 μM had no effect on the conductivity of bilayers regardless of the composition of the solutions bathing the BLM. For glycyrrhetic acid and **4** and **6**, a dose-dependent increase in the BLM conductivity was found starting at 2-5 μM in a medium containing K^+ (10 μM) at pH 7.4. Conductivity for other ions was not observed. The calculated specific conductivity curves for these compounds behave as saturation curves. This indicates that these compounds are ionophores (Fig. 4). The specific conductivity at concentrations greater than 4.2, 7.5, and 64 μM for glycyrrhetic acid, **4**, and **6** was 36, 61, and 27.2 pS, respectively. The greatest conductivity was observed for the glycyrrhetic acid derivative with piperidine.

Thus, DSC, EPR, and BLM unambiguously show that the studied compounds partially or fully penetrate into the hydrophobic region of a lipid bilayer. Compounds fully intercalated into the bilayer probably act as ionophores. The membrane activities of the studied compounds depend on the nature of the glycyrrhetic acid substituent. The biological effect of these compounds may appear because they change the structural organization of branched lipids of intact proteins that are needed for their normal functioning. However, further research is needed to understand fully the mechanism of action of the glycyrrhetic acid derivatives.

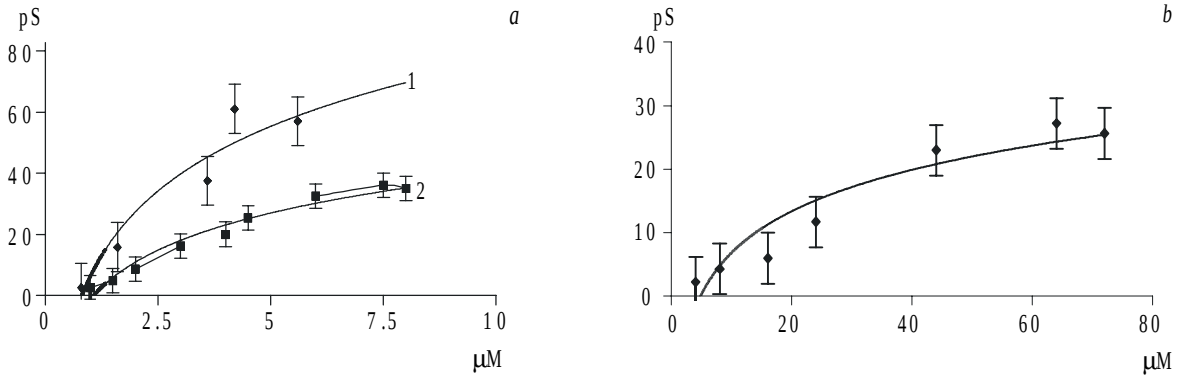

Fig. 4. Specific conductivity of BLM as a function of concentration of glycyrrhetic acid and its derivatives: glycyrrhetic acid (1) and **4** (2) (a) and **6** (b). Compounds were added to both sections of the experimental cell. Medium: KCl (10 mM), tris-HCl (10 mM), pH 7.4.

EXPERIMENTAL

PMR spectra were recorded in $CDCl_3$ and CCl_4 on an XL-100 (Varian, USA) instrument with TMS internal standard. PMR spectra of **2**, **4**, **5**, and **7** have been reported previously [8]. Chemical shifts of substituents bonded to the 3β-acetoxy-18βH-glycyrrhetic acid framework are given.

2-(N,N-Diethylamino)ethyl-3β-acetoxy-18-βH-glycyrrhetate (1). Yield 84.3%, mp 170-174°C, $C_{38}H_{61}O_5N$.

PMR (δ, ppm, J/Hz): 1.12 (6H, t, J = 7.1, CH_2–CH_3), 2.29 (1H, s, H-9), 2.4-2.8 (6H, m, N–CH_2), 2.75 (1H, br.d, J = 13.5, H_e-1), 4.06 (2H, t, J = 6.8, O–CH_2), 4.38 (1H, m, H-3), 5.57 (1H, s, H-12).

2-(N-Morpholinyl)-(1-methyl)ethyl-3-O-acetyl-18-βH-glycyrrhetate (3). Yield 81.4%, mp 204-206°C, $C_{39}H_{61}O_6N$.

PMR (δ, ppm, J/Hz): 1.24 (3H, d, J = 6.9, C–CH_3), 2.31 (1H, s, H-9), 2.4-2.72 (6H, m, N–CH_2), 2.75 (1H, br.d, J = 13.5, H_e-1), 3.78 (4H, m, OCH_2), 4.41 (1H, m, H-3), 5.06 (1H, m, O–CH), 5.58 (1H, s, H-12).

N-(3-β-Acetoxy-11,30-dioxo-18β-olean-12-en-30-yl)-anabasin (6). Yield 74.7%, mp 232-234°C, $C_{42}H_{60}O_4N_2$.

PMR (δ, ppm, J/Hz): 2.31 (1H, s, H-9), 2.75 (1H, br.s, J = 13.5, H_e-1), 2.81 (1H, m, H_a-6′), 4.08 (1H, m, H_e-6′), 4.37 (1H, m, H-3), 5.52 (1H, s, H-12), 5.70 (1H, m, H_a-2′), 7.14 (1H, dd, J_1 = 7.9, J_2 = 6.5, H-3″), 7.54 (1H, dt, J_1 = 7.9, J_2 = 1.8, H-4″), 8.30 (1H, dd, J_1 = 6.5, J_2 = 1.8, H-2″), 8.35 (1H, d, J = 1.8, H-6″).

N-(3-β-Acetoxy-11,30-dioxo-18β-olean-12-en-30-yl)-cytisine (8). Yield 78.9%, mp 246-249°C, $C_{43}H_{50}O_5N_2$.

PMR (δ, ppm, J/Hz): 2.2-3.2 (2H, m, H_a-11′ and H_e-13′), 2.36 (1H, s, H-9), 2.73 (1H, br.d, J = 13.5, H_e-1), 3.6-4.7 (4H, m, H_e-10′, H_a-10′, H_e-11′, and H_e-13′), 4.1 (1H, m, H-3), 5.68 (1H, s, H-12), 6.1 (1H, dd, J_1 = 7.5, J_2 = 2.0, H-3′), 6.47 (1H, dd, J_1 = 9.1, J_2 = 1.9, H-5′), 7.33 (1H, dd, J_1 = 9.1, J_2 = 7.5, H-4′).

2-(N-Cytisinyl)-ethyl-3-O-acetyl-18-βH-glycyrrhetate (9). Yield 76.3%, mp 278-281°C, $C_{45}H_{64}O_6N_2$.

PMR (δ, ppm, J/Hz): 2.33 (1H, s, H-9), 2.4-2.8 (6H, m, NCH_2), 2.79 (1H, br.d, J = 13.5, H_e-1), 3.6-4.4 (2H, m, H_e-10′ and H_a-10′), 4.10 (2H, t, J = 6.8, OCH_2), 4.40 (1H, m, H-3), 5.56 (1H, s, H-12), 6.07 (1H, dd, J_1 = 7.5, J_2 = 2.0, H-3′), 6.50 (1H, dd, J_1 = 9.0, J_2 = 2.0, H-5′), 7.33 (1H, dd, J_1 = 9.0, J_2 = 7.5, H-4′).

2-(N-Cytisinyl)-(1-methyl)ethyl-3-O-acetyl-18-βH-glycyrrhetate (10). Yield 72.7%, mp 296-298°C, $C_{46}H_{66}O_6N_2$.

PMR (δ, ppm, J/Hz): 1.27 (3H, d, J = 6.8, C–CH_3), 2.35 (1H, s, H-9), 2.3-2.7 (6H, m, NCH_2), 2.74 (1H, br.d, J = 13.5, H_e-1), 3.6-4.4 (2H, m, H_e-10′ and H_a-10′), 4.42 (1H, m, H-3), 5.1 (1H, m, OCH), 5.58 (1H, s, H-12), 6.05 (1H, dd, J_1 = 7.6, J_2 = 1.9, H-3′), 6.48 (1H, dd, J_1 = 9.1, J_2 = 2.0, H-5′), 7.35 (1H, dd, J_1 = 9.1, J_2 = 7.6, H-4′).

Colorless needle-like crystals of **8** were grown over three days by slow evaporation at room temperature of an acetone solution. A crystal of dimensions 0.25×0.10×0.10 mm was selected for the study. Unit-cell constants and the space group were determined and refined using 25 reflections on a Crystal-Logic diffractometer, which was a combination of a PC-controlled Syntex $P2_1$ diffractometer with a rotating-anode x-ray generator. The unit-cell constants are a = 13.580(4), b = 30.374(9), c = 11.139(3) Å, V = 4595(2) $Å^3$, Z = 4, ρ = 1.10 g/cm^3, space group $P2_12_12_1$, absorption coefficient μ = 0.598 mm^{-1}, and F(000) = 1652. Integrated intensities were measured by θ/2θ-scanning using Cu Kα-radiation and a graphite monochromator.

TABLE 3. Coordinates ($\times 10^4$) and Equivalent Thermal Parameters ($Å^2 \times 10^3$) for Nonhydrogen Atoms in **8**

Atom	x	y	z	U(eq)
N(1)	3355(4)	697(2)	16675(4)	65(1)
N(2)	1736(5)	79(2)	17757(5)	71(2)
C(1)	1528(4)	2489(2)	8795(5)	58(2)
C(2)	1358(4)	2768(2)	7671(6)	67(2)
C(3)	796(5)	3181(2)	7993(6)	73(2)
C(4)	-215(5)	3095(2)	8580(6)	71(2)
C(5)	-36(4)	2783(2)	9652(5)	58(1)
C(6)	-960(4)	2686(2)	10387(5)	62(1)
C(7)	-706(4)	2518(2)	11613(5)	59(2)
C(8)	-36(4)	2104(2)	11618(5)	51(1)
C(9)	818(4)	2169(2)	10694(5)	47(1)
C(10)	567(4)	2354(2)	9434(5)	51(1)
C(11)	1454(4)	1748(2)	10714(5)	45(1)
C(12)	1540(4)	1517(2)	11863(5)	50(1)
C(13)	1085(4)	1623(2)	12887(5)	50(1)
C(14)	409(4)	2037(2)	12913(5)	50(1)
C(15)	-398(5)	1987(2)	13854(5)	65(2)
C(16)	-55(5)	1784(2)	15039(5)	63(1)
C(17)	422(4)	1329(2)	14880(5)	56(1)
C(18)	1297(4)	1370(2)	14014(5)	49(1)
C(19)	2230(4)	1566(2)	14610(5)	55(1)
C(20)	2536(4)	1386(2)	15851(5)	54(1)
C(21)	1627(5)	1394(2)	16642(5)	65(2)
C(22)	759(5)	1147(2)	16082(6)	64(2)
C(23)	-943(5)	2913(3)	7637(7)	89(2)
C(24)	-609(6)	3543(2)	9037(8)	90(2)
C(25)	34(4)	2013(2)	8648(5)	60(1)
C(26)	1073(5)	2428(2)	13294(5)	61(1)
C(27)	-334(5)	1006(2)	14337(7)	74(2)
C(28)	-691(4)	1703(2)	11264(6)	61(1)
C(29)	3347(6)	1701(2)	16307(6)	77(2)
C(30)	2988(4)	917(2)	15701(5)	54(1)
C(31)	876(12)	4043(4)	5619(12)	162(5)
C(32)	1230(10)	3769(4)	6656(12)	129(4)
C(33)	3438(5)	837(2)	17905(5)	68(2)
C(34)	3090(6)	481(2)	18781(6)	73(2)
C(35)	3688(7)	63(2)	18606(7)	82(2)
C(36)	3530(6)	-78(2)	17311(7)	80(2)
C(37)	3872(7)	277(2)	16454(6)	80(2)
C(38)	1995(6)	384(2)	18607(5)	70(2)
C(39)	2457(7)	-204(2)	17118(7)	89(2)
C(40)	766(8)	-20(2)	17509(8)	92(2)
C(41)	67(7)	204(3)	18172(9)	102(2)
C(42)	320(8)	508(3)	19001(9)	103(3)
C(43)	1293(7)	599(2)	19233(7)	81(2)
O(1)	1896(3)	1611(1)	9845(3)	58(1)
O(2)	629(4)	3440(2)	6912(5)	92(2)
O(3)	3034(4)	754(1)	14708(4)	72(1)
O(4)	588(6)	-302(2)	16721(6)	124(2)
O(5)	1953(9)	3841(4)	7204(12)	198(5)
C(1A)	1720(30)	3825(11)	12000(40)	400(40)
C(2A)	2330(40)	3521(18)	11240(40)	300(20)
O(1A)	980(30)	3670(11)	12440(40)	380(20)
C(3A)	1960(70)	4298(17)	12250(100)	710(100)
C(1B)	2500(30)	3535(12)	12170(30)	300(50)
C(2B)	2460(50)	3454(19)	13500(30)	230(30)
O(1B)	2730(60)	3900(14)	11810(50)	330(40)
C(3B)	2270(20)	3185(11)	11260(30)	107(11)
O(1W)	-1200(30)	-333(9)	15630(30)	389(13)
O(2W)	2940(30)	4821(13)	6980(40)	510(20)

The stability of the crystal was monitored using three reference reflections after each 100 measurements. The experimental data set was collected at 293 K. The range of angles was $\theta = 2.91\text{-}58.52°$; indices, $-1 \le h \le 15$, $-33 \le k \le 33$, and $0 \le l \le 12$. The data set consisted of 3009 reflections after removing weak reflections with $I < 2\sigma(I)$. A total of 3675 reflections were collected. The structure was solved by direct methods using the SHELXS-86 programs [15] adapted for an IBM PC. The structure was refined by full-matrix least-squares techniques using the SHELXTL-97 programs [16]. H atoms were found geometrically and

refined using a riding model. The agreement factors after final refinement of the positional and thermal parameters were $R_1 = 0.075$ ($wR_1 = 0.213$), $R_2 = 0.083$ ($wR_2 = 0.235$). Coordinates of nonhydrogen atoms are listed in Table 3. The molecule was drawn using XP in SHELXTL-Plus [17].

DSC Method. Samples for multilamellar dispersions were prepared as described before [10]. Thermodynamic parameters of phase transitions of multilamellar dispersions were determined on a DASM-4 differential scanning microcalorimeter at 1°C/min.

EPR Method. We used benzo-γ-carboline as a spin probe. Its structure is:

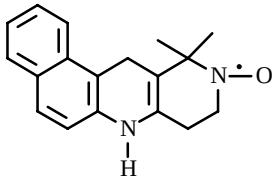

A solution in alcohol was added to the samples such that the probe concentration reached 4×10^{-5} M. Lipid samples from egg phosphatidylcholine were prepared by the literature method [11]. EPR spectra were recorded on a Bruker (Germany) radio-spectrometer at a modulation amplitude less than 1 G and a power on the resonator of less than 20 mW.

BLM Method. Bilayer lipid membranes were formed by the Montal-Mueller method [18] in apertures (diameter 0.35-0.40 mm) in screens (thickness 20 μm) of a Teflon two-chamber cell at 25±1°C. Lipid bilayers were prepared by placing lipid (azolectin) solution (10-15 μL, 0.5%) in octane. The *trans*-chamber of the cell was a virtual ground. The sign of the potential was determined relative to it. The current was taken as positive if cations migrated into this chamber. Derivatives of glycyrrhetic acid were added to both chambers at concentrations of 1-100 μM.

REFERENCES

1. G. A. Tolstikov, L. A. Baltina, E. E. Shul′ts, and A. G. Pokrovskii, *Bioorg. Khim.*, **23**, No. 9, 691 (1997).
2. R. Kh. Gayanov, H.-O. Kim, M. I. Goryaev, and M. P. Irismetov, *Zh. Obshch. Khim.*, **46**, 2375 (1976).
3. M. V. Whitehouse and J. M. Haslam, *Nature (London)*, **196**, 413 (1962).
4. H. Bastrom, K. Berusten, and M. W. Whitehouse, *Biochem. Pharmacol.*, **113**, 413 (1964).
5. H. Inoul, H. Saito, Y. Koshihara, and S. Murota, *Chem. Pharm. Bull.*, **34**, 897 (1986).
6. M. Kimura and J. Kimura, *Jpn. J. Pharmacol.*, **39**, 387 (1985).
7. K. Iton, T. Hara, T. Shiraishi, T. Taniguchi, S. Morimoto, and T. Onishi, *Biochem. Int.*, **18**, 442 (1989).
8. D. N. Dalimov, A. Zh. Zhuraev, and F. G. Kamaev, *Khim. Prir. Soedin.*, 129 (2001).
9. L. Parkanyi, *RING Program for Conformation Analysis*, Budapest (1979).
10. T. F. Aripov, I. A. Rozenshtein, B. A. Salakhutdinov, A. A. Lev, and V. A. Gotlib, *Gen. Physiol. Biophys.*, **6**, 343 (1987).
11. T. F. Aripov, B. A. Salakhutdinov, Z. T. Salikhova, A. S. Sadykov, and B. A. Tasmukhamedov, *Gen. Physiol. Biophys.*, **3**, 489 (1984).
12. B. A. Salakhutdinov, E. T. Tadzhibaeva, M. V. Zamaraeva, I. I. Tukfatullina, T. F. Aripov, L. G. Mezhlumyan, E. F. Redina, and P. Kh. Yuldashev, *Khim. Prir. Soedin.*, 82 (1998).
13. M. Mousseron-Conet and F. Granzet, *Bull. Soc. Chim. Fr.*, 4668 (1967).
14. L. Kh. Khalilov, E. V. Vasil′eva, A. A. Fatikhov, and G. A. Tolstikov, *Khim. Prir. Soedin.*, 363 (1991).
15. G. M. Sheldrick, *Acta Crystallogr. Sect. A: Found. Crystallogr.*, **46**, 467 (1990).
16. G. M. Sheldrick, *SHELXTL-97, Program for the Refinement of Crystal Structures*, University of Gottinggen, Germany (1997).
17. Siemens XR, *Molecular Graphics Program*, Version 5.03, Siemens Analytical X-ray Instruments Ins., Madison, Wisconsin (1994).
18. M. Montal and P. Mueller, *Proc. Natl. Acad. Sci. USA*, **69**, 3561 (1972).